Title
Effects of co-solvents on peptide hydration water structure and dynamics

Journal
Physical Chemistry Chemical Physics, 12(2)

ISSN
0956-5000

Authors
Johnson, Margaret E
Malardier-Jugroot, Cecile
Head-Gordon, Teresa

Publication Date
2010-01-14

DOI
10.1039/b915888j

Peer reviewed

Effects of Co-Solvents on Peptide Hydration Water Structure and Dynamics

Margaret E. Johnson[1,2,3*], Cecile Malardier-Jugroot[4], and Teresa Head-Gordon[1,2,3*]

[1]*UCSF/UCB Joint Graduate Group in Bioengineering*

[2]*Department of Bioengineering, University of California, Berkeley*

[3]*Physical Biosciences Division, Lawrence Berkeley National Laboratory*

Berkeley, California 94720 USA

[4]*Department of Chemistry and Chemical Engineering, Royal Military College of Canada, Kingston, K7K 7B4, Canada*

We evaluate the molecular response of hydration water as a function of temperature and proximity to the surface of the peptide N-acetyl-leucine-methyl-amide (NALMA) when in the presence of the kosmotrope co-solvent glycerol or the chaotrope co-solvent dimethyl sulfoxide (DMSO), using molecular dynamics simulation with a polarizable force field. These detailed microscopic studies complement established thermodynamic analysis on the role of co-solvents in shifting the equilibrium for proteins away from or towards the native folded state. We find that the structure of the water at the peptide interfaces reflects an increase in hydration number in the glycerol solution and a decrease in hydration numbers in the DMSO solution. While the water dynamics around NALMA in the presence of both co-solvents is slower than that observed with the water solvent alone, in the DMSO mixture we no longer measure a separation in water motion time scales at low temperatures as is seen in the pure water solvent, but rather one single relaxation time. In the glycerol, however, we do observe a separation of time scales at low temperatures, supporting the hypothesis that hydration water near a hydrophobic solute evolves on a separate time scale than the extensive hydrogen bonding network of more bulk-like water. Our simulation studies highlight the differences in the two co-solvent solutions due to the relative frequency of water contacts with the hydrophobic vs. hydrophilic peptide surface, and direct water interactions with the co-solvents.

INTRODUCTION

Small molecule co-solvents occur naturally in cellular environments, and are therefore important components of solutions for *in vitro* studies of protein folding and functioning. Not only can their inclusion be necessary to prevent spurious aggregation of proteins[1,2], but these additives are important for the design of new biomolecules[3] and control of protein self-assembly or denaturation[4]. Compared with solvating a folded protein in pure water, the co-solvent can either shift the protein equilibrium towards the denatured state, the functional native state, or have a neutral effect[5,6], which may depend on the particular protein, concentration, temperature, pH and pressure.

The behavior of the protein-water-co-solvent system is best described as a weakly interacting system[5], and a thermodynamic theory of such three component systems was first developed decades ago to describe the macroscopic response of the protein-water system to the introduction of a third co-solvent molecule[7-9]. Protein stabilizers may increase the free energy of both the folded and unfolded state relative to the pure water solvent, but the free energy increase is larger for the unfolded state, thereby stabilizing the folded state when the co-solvent is present[5,6]. Despite this foundation on the macroscopic thermodynamic properties of weakly interacting systems, the validity of various models or assumptions used to explain observed experimental results is still not fully resolved[10]. Notably, these theories do not fully describe the molecular mechanism by which the co-solvents interact with the hydration water or protein surface to facilitate or prevent protein folding reactions.

Furthermore, a thermodynamic description does not describe the dynamical nature of the solution constituents that are important factors in protein function, which requires conformational flexibility of the native protein. For instance, moderate concentrations of DMSO have been shown to actually enhance enzyme activity by increasing the conformational flexibility of the protein[11], while additives that stabilize proteins may also decrease their functionality by decreasing conformational flexibility[12]. Equally important is the participation of water solvent in protein function[13], although the role of hydration water *dynamics* in protein function is a matter of current research. Studies have demonstrated that proteins do not function at low temperatures at which they do not have sufficient vibrational flexibility[14], and further studies suggest that the onset of increased protein fluctuations at higher temperatures may be coupled to the temperature dependence of the underlying water dynamics[15-17]. Molecular dynamics studies of proteins in glycerol observe a similar coupling

between protein and the glycerol solvent dynamics[18]. Several studies have demonstrated that rotational and translational dynamics of hydration water is slowed compared to bulk[19], and that this perturbation to the water dynamics extends out several diameters beyond the first hydration layer[20,21], whereas structural perturbations extend only to water in contact with the protein[19,22].

In this work we simulate three component solution systems to provide new insights into the microscopic structural and dynamical behavior of water in such environments. The two co-solvent molecules we investigate here are the highly polar glycerol, and the amphiphilic DMSO. Glycerol is a known protein stabilizer[23,24] that can prevent proteins from denaturing at low temperatures or aggregating under long-term storage[1]. In fact, proteins can both fold and remain active in almost pure glycerol[25]. DMSO is a versatile additive, commonly used as a solvent buffer at low concentrations[26], but acting as a denaturant for most proteins at high concentrations[27], such as the 1:4 DMSO:H_2O concentration used here. For instance, proteins solvated in pure DMSO solvent cannot exhibit functional activity due to their inability to adopt their native folded structure[25]. Experimental evidence suggests that DMSO denatures folded proteins by excluding water molecules from the protein surface, while glycerol stabilizes the folded protein by increasing water at the surface, a phenomenological description of co-solvent behavior known as preferential hydration[5]. Given the polar nature of the glycerol molecule and the amphiphilic nature of the DMSO molecule, we consider in this study to what extent the structure and dynamics of the water at the protein surface varies along the hydrophobic vs the hydrophilic regions of a small model peptide. We thereby isolate the effects of the co-solvents as a function of the peptide surface chemistry to provide new mechanistic insight over results that average across the full folded protein surface.

In a series of experimental and molecular simulation studies on concentrated peptide solutions[28-33], we have previously characterized the properties of water hydrating both hydrophilic NAGMA (N-Acetyl-Glycine-methyl-amide) and amphiphilic NALMA peptides as a function of temperature and proximity to the peptide surface. The high peptide concentrations we use here provide a model of overlapping hydration shells near protein surface amino acids, whereas dilute concentrations of these same peptides measured by recent NMR experiments are more representative of the hydration dynamics of more extended polypeptide chains[34]. Using quasi-elastic neutron scattering (QENS) and molecular dynamics (MD) simulation we determined that the amphiphilic NALMA peptide

solution gives rise to two translational relaxations for the water dynamics, due to having an inner hydration layer of water that interacts with the amphipathic peptide surface on a longer timescale than the outer hydration layer that interacts mostly with other hydrogen bonding water molecules[28]. By contrast, the NAGMA peptide solution showed only a single non-Arrhenius translational process with no distinction between hydration layers, as the dynamics of all hydration layers evolve on the same timescale for this hydrophilic peptide[29]. These results highlighted the perturbations to hydration water dynamics arising from the amphiphilic nature of a protein surface. Given our comprehensive analysis of the solution of 1M NALMA in pure water, this provides a foundation for measuring the perturbations to the structure and dynamics that occur at the peptide surface of three component systems when in the presence of the co-solvents glycerol and DMSO. In particular, we analyze the structure of the water around the solutes and co-solvent molecule, and any displacement of water molecules from the peptide surface relative to the pure water solution, to compare with experimental expectations on preferential hydration[5] in the two solutions. We also analyze the dynamics of subpopulations of water in the solutions as a function of distance from the peptide surface, to provide a more detailed microscopic description of the effects of the co-solvent chemistry on the hydration water dynamics. We validate our simulations with recent experimental data on the structure and dynamics of these systems obtained from neutron diffraction and quasi-elastic neutron scattering, respectively[35].

METHODS

Simulation Models and Protocols

In accord with our experimentally prepared solutions[35], our simulations maintain a constant mole ratio of 1 NALMA:55 solvent molecules (~1M), and co-solvent ratios of 5:1 H_2O:Glycerol, and 4:1 H_2O:DMSO. Our MD simulations were run using the polarizable AMOEBA force field[36] for water and proteins, implemented in parallel in the AMBER simulation package with Coulomb interactions described by Particle Mesh Ewald[37]. Both three-component solutions were simulated with 32 NALMA peptides, with the H_2O:Glycerol solvent comprised of 1467:293 molecules, and the H_2O:DMSO solvent comprised of 1408:352 molecules. The Beeman algorithm with a timestep of 1fs was used to numerically integrate the equations of motion. The diffusion of the NALMA solutes in these viscous solvents was extremely slow; to avoid biasing our results due to the choice of the initial distribution of NALMA solutes, three distinct initial configurations of NALMA solutes were

generated from a temperature of 400K at which they were able to diffuse much more freely. These three configurations were propagated independently for each temperature to provide a better sampling of solution conditions. Simulations were carried out at the temperatures 298K, 288K, 277K, 271K, 263K, 255K. For each temperature, simulations were initially run in the NPT ensemble for 0.5-2ns to equilibrate the box size to a pressure of 1atm using the (default) Berendsen barostat. We then performed NVT simulations at the determined density, using the Berendsen thermostat[36] with equilibration times between 1.0-2.0ns, with longer times used for lower temperatures. The NVE ensemble was used to collect all of the dynamics data, with initial equilibrations from 0.6-1.0ns, followed by production runs of 4.0-6.0ns. The NVE runs were run with the induced dipole iterative tolerance value set at 1E-5, instead of the default 1E-2. Additional NVE simulations were run for 2ns at 263K, where configurations were saved every 20fs for the population analysis. At the highest temperatures (298K and 288K) we also ran simulations using the AMOEBA-V parameters for the water molecules[38]. However, the resulting dynamics were statistically no different than results using the standard AMOEBA water parameters, so we report all results for the standard AMOEBA water molecule parameters. Control simulations were also run for a system of 1:4 DMSO:H_20 and 1:5 Glycerol:H_2O without any NALMA peptides present. These simulations had 100 co-solvent molecules, and 400 and 500 water molecules, respectively. They were equilibrated in the same manner as noted above and run at the temperatures 298K, 288K, 277K, 271K, and 263K.

Molecule Parameterization

Force field parameters were not directly available for the glycerol and DMSO molecules for use with the AMOEBA force field, and required calculations to derive parameters for the force constants and equilibrium geometric values for bond stretch, bond angle, coupled bond stretch-bend, and torsions, as well as the nonbonded Lennard-Jones (LJ) parameters and atom centered multipole moments up to quadrupole[39]. The atomic polarizabilities were kept the same as the values used for all atoms in the AMOEBA force fields. To construct parameter sets, we generated initial optimized configurations of these molecules using *Gaussian03*[40] at the level of MP2/aug-cc-pVTZ. The necessary multipole moments were measured from the optimized wave functions using the distributed multipole analysis (DMA)[41] and software of A. Stone[42]. Following the protocol of Ren and Ponder[43], the effects of intramolecular polarization between dipole moments was removed using the TINKER software package, since our molecules are large enough to allow for intramolecular

polarization, similar to the alanine-dipeptide described in Ref.[43]. For glycerol, the groups whose members could not polarize from the permanent multipoles of each other were designated as each of the OH groups, the two CH groups, and the CH2 group. For DMSO, the methyl groups were each separate, as was the SO group. In analogy with the water molecule parameters, the magnitude of the OH quadrupole moments were decreased by a factor of 40%[36]. For chemically equivalent molecules (e.g. the methyl hydrogens), the multipole moments in the local coordinate frame were averaged. The multipole moments were also averaged across two different optimized geometries to better capture different conformations of the molecules.

The Lennard Jones (LJ) parameters for the atoms were taken from analogous molecules parameterized for the AMOEBA force field available in the TINKER software package, as were the bond and angle force constants. In the case of DMSO, an additional lone pair site was added to act as a local reference frame for the sulfur atom. This 'ghost' site has no multipole moments or LJ parameters, but only a bond and angle constraint to keep it constrained geometrically off the sulfur atom. For DMSO, bond and angle force constants were taken from the polarizable MM3 force field[44] (consistent with AMOEBA force field parameterization) available with the AMBER package[37]. Lastly, the torsion coefficients were evaluated by rotating each molecule around the given torsion angle, and re-optimizing the geometry with that angle constrained. For each torsion angle, MP2/6-311G** calculations using QChem[45] were used to optimize the geometry around that constrained angle and evaluate the energy. The torsion coefficients for the AMOEBA force field were varied to best reproduce the quantum energy profile as a function of torsion angle. The totality of AMOEBA parameters for DMSO and glycerol are available in the Supplementary material.

Dynamical observables

The translational diffusion coefficient of the water was obtained from the simulations by calculating the mean square displacement (MSD) of the particles, and using the Einstein relation

$$D_t = \frac{1}{6}\lim_{t\to\infty}\frac{d}{dt}\left\langle \left|\mathbf{r}(t)-\mathbf{r}(0)\right|^2 \right\rangle \qquad (1)$$

where ***r(t)*** is the position vector of each atomic center at time *t*, and the angled brackets indicate and average over the ensemble of configurations at the simulated volume. The convergence of the diffusion constant at long times was verified by calculating the slope of the MSD over multiple different time intervals (between the range 0.6 to 5 ns depending on temperature) to ensure the

linear regime had been reached. The diffusion constants as a function of temperature T are fit with the Arrhenius function,

$$D = D_0 \exp\left(\frac{E_A}{k_B T}\right) \tag{2}$$

where E_A is a temperature independent activation energy, k_B is boltzmann's constant, and D_0 is a reference timescale for the T-->∞ limit.

We also evaluate the self-intermediate scattering function (ISF) for the water hydrogen atoms (the same as the QENS experimental observable):

$$F_s^H(Q,t) = \left\langle \exp\{i\mathbf{Q}\cdot[\mathbf{r}_H(t) - \mathbf{r}_H(0)]\}\right\rangle \tag{3}$$

where Q is the momentum transfer and $\boldsymbol{r_H(t)}$ is the position vector of each hydrogen center. This allows for direct comparison with the QENS observables without resorting to more approximate QENS models. We find that fits to the ISF deviate significantly from a single exponential decay expected from systems obeying simple Fickian diffusion, even approaching the low Q hydrodynamic regime[46]. To quantify this deviation, we fit the ISF with a stretched exponential function

$$A\,exp\left[-\left(\frac{t}{\tau}\right)^{\beta}\right] \tag{4}$$

where τ is the timescale of relaxation, and values of β less than one indicate a more complex mechanism for relaxations, seen for instance in systems obeying hierarchical dynamics and in glass-forming systems[47]. The average relaxation time for a stretched exponential depends on both τ and β, so to quantify a single value for comparison between solutions, we use the following expression due to Chen and coworkers[48]:

$$\overline{\tau} = \int_0^{\infty} dt \exp\left[-\left(\frac{t}{\tau}\right)^{\beta}\right] = \frac{\tau}{\beta}\Gamma\left(\frac{1}{\beta}\right). \tag{5}$$

We evaluate the rotational correlations with the rotational ISF

$$F_R^H(\boldsymbol{Q},t) = \left\langle exp(-i\boldsymbol{Q}\cdot\boldsymbol{b}(0)\,exp(i\boldsymbol{Q}\cdot\boldsymbol{b}(t)\right\rangle = \sum_0^{\infty}(2l+1)j_l^2(Qb)C_l(t) \tag{6}$$

where the second term on the right of Eq. (7) is the exact expansion due to Sears[49]. The vector $\boldsymbol{b}$ is the vector connecting the center of mass to a hydrogen atom, and the lth order rotational correlation functions are given as

$$C_l(t) = \left\langle P_l(\boldsymbol{b}(0) \cdot \boldsymbol{b}(t)) \right\rangle \quad (7)$$

where P_l is the lth order legendre polynomial, and in which only terms up to l=2 make significant contributions for the Q<2Å^{-1} range studied[50].

Population analysis

In order to evaluate the dynamics of different populations of water, we delineate two regions on the peptide surface such that we can distinguish between water solvating the hydrophilic backbone atoms (O and N atoms), and hydration water that solvates the hydrophobic side chain carbons. As explained previously[28], the cutoff for the backbone nitrogen and leucine carbons is chosen at 4.0Å, and 3.0Å for the backbone oxygens. We saved configurations every 20 timesteps to keep track of the domain the water molecules resided in, using a larger time window to smooth small motions in and out of the regions. By establishing these two surface domains, the water molecules as a function of a time interval Δt can be characterized in four different ways: water molecules that remain at the hydrophobic surface for the entirety of Δt, those that remain at the hydrophilic surface for the entirety of Δt, those that remain in the bulklike region (outside of these surface regions) for the entirety of Δt, and those waters which at some point in Δt travelled from one region to another. The weighted average over the individual correlation functions of these water populations can then be used to regenerate the full water average via:

$$\left\langle \left|\mathbf{r}(t+\Delta t) - \mathbf{r}(t)\right|^2 \right\rangle = \sum_{i=1}^{\mathrm{Re}\,gions} P_i(\Delta t) * \left\langle \left|\mathbf{r}_i(t+\Delta t) - \mathbf{r}_i(t)\right|^2 \right\rangle_i \quad (8)$$

The percentages, $P_i(\Delta t)$, reflect both the propensity to stay within a region i, as well as the average size of surface vs. bulk populations. The probability of a water molecule remaining isolated within either the surface or bulklike regions inevitably drops as time evolves, whilst conversely the probability of having transferred must increase as time evolves. The crossover at longer times of the majority of water molecules into this 'transferred water' population reflects a degree of exchange between the surface and bulk-like regions. We also generalize Eq. (3) and (6) using the same regional analysis for calculation of distinct contributions to the ISF.

Hydrogen bonding population relaxation. We additionally evaluate the relaxation time of hydrogen bonds formed between water molecules, between water and co-solvent molecules, and between water and NALMA peptides by calculating the auto-correlation function,

$$B(t) = \frac{\left\langle \sum_{i}^{Nhbonds} h_i(t) h_i(0) \right\rangle}{\left\langle \sum_{i}^{Nhbonds} h_i(0) \right\rangle} \tag{9}$$

which is unity at time 0, and h_i=1 if the bond *i* exists and h_i=*0* otherwise. This correlation function only reflects the breaking of hydrogen bonds as time progresses, excluding the formation of any new bonds. We use a geometric definition[51,52] where an OH—O hydrogen bond is considered to exist if the oxygen-oxygen distance is <3.5Å and the angle between OH—O is >150 degrees. This definition is also used for the water-solute hydrogen bonds, where the average O-O separation is similar to that between water molecules: the peaks in $g_{OO}(r)$ between water and glycerol, between water and DMSO, and between water and NALMA are 2.8Å, 2.7Å, and 2.8Å respectively. For water-water interactions, we test the four possible hydrogen bonds between a given pair; for water-solute interactions, we separately evaluate the hydrogen bond correlation functions for water molecules donating protons vs. where water is a proton acceptor where applicable.

Orientational Structure

For structural comparison, we calculate the radial distribution function $g_{MM}(r)$, where M refers to an arbitrary label, as well as the full angular pair correlation function defined by

$$g_{OM}(r,\theta,\varphi) = \left\langle \frac{N_O(r,\theta,\varphi)}{\int_{r1}^{r2} r^2 dr \int_{\varphi 1}^{\varphi 2} \sin(\varphi) d\varphi \int_{\theta 1}^{\theta 2} d\theta} * \frac{V_{tot}}{N_M N_{Wat}} \right\rangle \tag{10}$$

where r, ϕ, and θ are the centers of the volume elements defined by dr, dϕ, and dθ, $N_O(r,\phi,\theta)$ counts up the number of water oxygens measured in that volume element, and the histogram is normalized by the number of reference atoms to water oxygen pairs in the total volume. A g_{OM} value of 1 reflects the average density of water in the solution.

RESULTS

Solution Structure in the presence of co-solvents

In order to characterize any clustering of the NALMA solute molecules in water or in the presence of a given co-solvent, the intermolecular $g_{CC}(r)$ between the carbons of the NALMA molecules at 298K is plotted in Figure 1, where the density approaches the average value of one expected at long distances for a homogeneous solution. These results confirm that there is no clustering between

NALMA solute molecules in solution, consistent with previous X-ray[53] scattering studies without additives, and consistent with our recent neutron diffraction studies in the presence of co-solvents[35].

We next determine the structural organization of water around the NALMA solute to determine how it changes in the presence of the DMSO or glycerol co-solvent. Our recent neutron diffraction studies showed that the DMSO co-solvent disrupted the contacts between water and the carbonyl group of the NALMA backbone[35]. Furthermore, the neutron diffraction experiments at 298K found a peak in $g_{HO}(r)$ at 1.8A in the pure aqueous 1M NALMA solution, consistent with a water-peptide hydrogen-bond, which is maintained in the 1M NALMA in 1:5 glycerol:H_2O solutions but disappears in the 1M NALMA in 1:4 DMSO:H_2O solution. Figure 2, however, shows that all three simulated solutions maintain the hydrogen bond between the solute C=O group and the water hydrogens, such that the presence of DMSO does not affect interactions between water and NALMA along the backbone as indicated by experiment.

However, the largest difference in water organization in the immediate hydration layer near NALMA in the presence of the glycerol vs. DMSO co-solvent occurs near the hydrophobic leucine side chain. Figure 3 shows that the glycerol solution gives rise to an increase in water molecules at the side chain interface (preferential hydration), while the DMSO co-solvent causes a noticeable decrease in water density near the hydrophobic group compared to the pure water solution. This is reasonable since the non-polar methyl groups of the DMSO molecule can orient towards the hydrophobic side chain, thereby minimizing the interactions with the polar water molecules and increasing the more favorable interactions between water molecules. This important result agrees with empirical evidence that stabilizing agents preferentially increase the hydration of the protein surface, while denaturants act to decrease hydration at the protein surface[5], with our results suggesting that this change is more pronounced at the exposed hydrophobic regions in the case of the DMSO co-solvent.

Figure 4 shows that the water structural correlations maintain a tetrahedral network in both of the co-solvent:H_2O:NALMA solutions, as is seen in the pure H_2O:NALMA solutions. This result is consistent with neutron diffraction studies of DMSO:H_2O mixtures at 1:3.7 concentrations (very close to our 1:4 concentration) which found that the water structure is not strongly affected by the presence of the DMSO, but that the water molecules form new hydrogen bonds with the DMSO[54],

which are slightly stronger, making the network somewhat stiffer[55]. The locations of the neighboring water molecules are slightly sharpened in the presence of co-solvent, as we see the maximum density reached is higher for the glycerol:H_2O:NALMA solution, and highest for the DMSO:H_2O:NALMA solution. This sharpening is similar to what is seen in the pure H_2O:NALMA solution as the temperature is lowered. In data not shown, we also calculated the orientational water density (Eq. 10) around a central water molecule out to the second hydration layer (6.4Å from the central oxygen). The simulations show good agreement with the orientational water structure in the pure H_2O:NALMA solution seen in the companion neutron diffraction data[35]. The simulations also reproduce the experimentally observed decrease in second hydration layer water density upon the addition of glycerol to the H_2O:NALMA solution. However, in the DMSO:NALMA:H_2O solution, we again find that the simulation maintains hydrogen bonding structure out to the second hydration shell that are found to be destroyed in the experimental characterization. Similar to the structural data observed at the peptide carbonyl bond group (Figure 2), these spatial density results imply that the DMSO is not able to consistently disrupt the interactions between water and other polar groups. As we note further below, this suggests that the DMSO molecule could be better parameterized. However, as is clear from Figure 3, the general amphiphilic nature of the DMSO is properly reflected in the simulations, as the DMSO successfully competes with water to prevent an unfavorable water-nonpolar interface around the leucine side chain.

Further, we also find through the orientational structural analysis (Eq. 10) that both the DMSO and the glycerol engage in hydrogen bonding with the water. In Figure 5 we display the radial distribution function between co-solvent oxygens and water oxygens, which shows a peak at a typical hydrogen bonding distance, consistent with the orientational distribution of co-solvent oxygens around a central water molecule (Figure 4) in which the co-solvent oxygens were very highly localized around the water hydrogens, forming a linear (hydrogen) bond between OH—O for both co-solvents.

In summary, the water structure remains tetrahedrally coordinated in the first hydration shell for all three solutions, and can form additional hydrogen bonds with both co-solvents. While the simulated structure is not fully in agreement with the experimental observations, the simulations yield the qualitatively correct result that the DMSO co-solvent depletes the hydration layer around the peptide, while the glycerol co-solvent is excluded from the peptide surface and therefore enhances

the hydration water density. This distinction will prove to be important in the comparison of the water dynamics for the kosmotrope vs. chaotrope co-solvents.

Water dynamics near NALMA in presence of co-solvents

Figure 6 reports the simulated translational diffusion coefficients of water as a function of temperature for the 1:4 DMSO:H_2O solution and the 1M NALMA in 1:4 DMSO:H_2O solution compared with our recent QENS data on the same systems[35]. Although the simulated self-diffusion constants are an order of magnitude slower than that observed experimentally for both systems, the theoretical model qualitatively reproduces the same Arrhenius temperature dependence, consistent with previous results on water-DMSO mixtures[55] (at a 1:2 concentration) and our recently reported QENS data[35]. Furthermore, adding NALMA to the DMSO:H_2O solution causes only a small decrease in the water diffusion constant and a small increase in the activation energy, consistent with experiment; for simulation the activation energy increases from 11.9 to 12.0 kcal/mol with the addition of NALMA, while for experiment the activation energy increases from 6.5 to 7.0 kcal/mol.

Figure 7 reports the simulated translational diffusion coefficients of water as a function of temperature for the 1:5 glycerol:H_2O and 1M NALMA in 1:5 glycerol:H_2O solutions compared with experiment. Again, the simulations are qualitatively consistent with experiment, with both glycerol solutions measuring a water self-diffusion with an Arrhenius temperature dependence down to 263K. The addition of NALMA to the glycerol:H_2O solutions causes a slight decrease in diffusivity in both experiment and simulation, and the activation energy actually decreases with the addition of NALMA; for the simulation the activation energy decreases from 11.8 to 11.2kcal/mol with the addition of NALMA, whereas experimentally the activation energy from 298K to 263K decreases from 7.3 to 5.7 kcal/mol. Notably, Figure 7 shows that the experimental analysis of the NALMA:glycerol:H_2O solution, much like the pure NALMA:H_2O solution previously characterized[28,30], exhibits two separate time scales at the lowest temperatures, whose origin we investigate through simulation.

In order to characterize the translational motions in the 1M NALMA in 1:5 glycerol:H_2O solutions simulations more carefully, we evaluate and analyze the intermediate scattering function (ISF) (Eq. 3) as we did in previous studies for the 1M aqueous NALMA solution[28]. The short time decay of the ISF correlations is due to the initial ballistic motion as well as decorrelation from the rotational

motion of the waters, while the longer time decay is due to translational diffusion. Analysis of the long time decay of the ISF for *all* solutions, even at the highest temperature and the lowest Q values studied, is shown to deviate from a single exponential decay. By fitting with a stretched exponential, Eq. (6), one can evaluate to what extent the system deviates from the expected exponential behavior of a system obeying Fickian diffusion. In Table 1 we compare the fit parameters for both co-solvent solutions with and without NALMA for T=298K and T=263K. Figure 8 plots the ISF for the glycerol:H_2O solution and the 1M NALMA in glycerol:H_2O solution along with the best fits to the stretched exponential function; the deviation of β from 1 shows that the mechanism for water translational relaxation is more complex than simple diffusion for the peptide and glycerol solution.

Population Dynamics

In order to investigate the possible origins of the separate time scales that was observed for only the 1M NALMA in glycerol:H_2O solutions, we evaluate the dynamical properties of the water molecules in different layers around the peptide. Figure 9 displays the time evolution of water in the outer hydration layers (referred to henceforth as "bulk-like", although it is still distinct from true bulk water) and the water that exchanges with the surface regions. The curves show the percentage of water molecules found in each region after a time Δt, as defined in Eq. (9), as a function of temperature. The plots reflect the rapidity of exchange between the two regions; the more readily the bulk-like water mixes and exchanges with the surface areas, the faster its curve crosses below the transfer water curve. These results show that the co-solvents are similar in their exchange rates at higher temperatures, but as the temperature lowers, the water in the DMSO solution remains separated for longer times compared to the glycerol solution. This could be because the DMSO excludes the water molecules from the peptide surface, so there is less surface volume for them to transition into, and it is more probable that they remain in the bulk.

In Figures 10 and 11 we plot the dynamic correlation functions for the different populations of water molecules for both the glycerol and DMSO solutions; Figure 10 plots the MSD, while Figure 11 shows both the translational and rotational (with l=1) ISF auto-correlation functions. We see that for the glycerol solutions (Figure 10a and 11a), there is a noticeable separation in the curves describing the bulk-like water compared to the water traveling in and out of the surface regions (labeled bulk and transfer, respectively). Figure 10a shows that the bulk-like water is diffusing slower than average and the surface exchange water is faster than average, consistent with Figure

11a in which we see that both the translational and rotational auto-correlation functions of the bulk-like water has a slower relaxation time, while the surface exchange water has a faster relaxation time. For the DMSO co-solvent however, the bulk-like water and the surface transfer water curves are nearly indistinguishable for all three calculated correlation functions (Figures 10b, 11b), aside from the only temporary separation for the rotational correlation. The water molecules that are trapped for their lifetimes at the peptide surface (labeled hydrophilic) have slow relaxation in all solutions, but they are a very small population that contributes very little to the average total signal and as such cannot explain a separation in time scales. Together, the two populations of bulk-like and transfer water provide nearly all the contribution to the observed average signal, indicating that these two populations are the sources of the two time scales observed in glycerol, and consistent with the lack of observation of two timescales for DMSO. These dynamic trends calculated from well-defined water populations are highly consistent with results found when performing the same analysis on water dynamics in a 1M NALMA vs 1.5M NAGMA solution[28], and therefore strongly suggest that these defined regions are reliable sources for the distinct time-scales measured experimentally.

Lastly, we evaluate the relaxation of hydrogen bonding populations in both solutions to further illuminate the possible mechanism by which the glycerol solution generates two separate timescales, and has a slower relaxation for water in the bulklike region, unlike that observed for the DMSO co-solvent. In Figure 12 we plot the average decrease in hydrogen bonds of a given initial configuration, normalized by the average number of hydrogen bonds formed at a given time. The three curves correspond to water molecules donating hydrogen bonds to the co-solvents, the NALMA, and forming bonds with other water molecules (see Methods). It is clear that the qualitative trends are similar in both solutions, where the longest lived hydrogen bonds are formed between water and co-solvents, followed by water and NALMA, and water to water; hydrogen bonds where the water oxygen accepts bonds from the NALMA or glycerol were less frequent and shorter lived (data not shown). The similarity between the two solutions suggests that it is not the hydrogen bonding lifetimes that gives rise to the separation in time scales observed only in glycerol. Indeed, evaluation of the regional water-water hydrogen bond correlation functions in the glycerol solution indicate the bulk-like water-water hydrogen bonds actually decorrelate slightly faster than the average! While the long-lived hydrogen bonds formed between the water molecules and the co-solvents can drive a measurable slow-down in the water dynamics away from the peptide surface

compared to the same solution without co-solvent, this hydrogen bonding analysis cannot distinguish the unique behavior observed only in the glycerol solution.

DISCUSSION AND CONCLUSIONS

In this paper we show that our computer simulations of water-peptide solutions with either glycerol or DMSO co-solvents qualitatively reproduce their distinct structural and dynamic properties known from experiment. Structurally the simulations reproduce experimental evidence that water maintains a tetrahedral organization in all solutions, which is corroborated in different experimental studies[35,54]. The structure of the 1M NALMA solution with 1:5 glycerol:H_2O solvent resembles the 1M NALMA solution with pure water solvent at the hydration surface of the peptides, except with an increase in water density. For the 1M NALMA solution with 1:4 DMSO:H_2O solvent, however, the hydration water structure is altered from pure water solvent, such that now the DMSO replaces the water at the peptide surface, most notably around the hydrophobic leucine residue. Our general measurement of an increase of surface hydration with addition of glycerol, and a decrease in water hydration with addition of DMSO is in good agreement with previous experimental evidence on preferential hydration[5].

This reasonable result stems from the chemical nature of the two co-solvent species. The polar glycerol molecule does not compete as effectively with the water molecules for contacts with the hydrophobic residue, while the amphiphilic DMSO molecule can form interactions with the hydrophobic surface of NALMA in a classic case of the hydrophobic effect. However, water maintains contact in both solutions with the hydrophilic peptide backbone surface, while in experiment, the water to carbonyl oxygen contact is disrupted in the H_2O:DMSO solvent. This discrepancy between our findings using neutron scattering vs. simulation could indicate that the parameters for our co-solvent molecules could be better optimized; in fact the strong directionality and the considerably longer hydrogen-bonding lifetime between water and co-solvent could also explain why the diffusion constants of solutions with co-solvents are all an order of magnitude slower than the experiments. Nevertheless, the qualitative structural and dynamical trends for all evaluated systems are consistent with the experimental results.

The changes in water structure at the peptide surfaces in the two solutions are accompanied by distinct dynamic correlation times in the two solutions. For the 1M NALMA in DMSO:H_2O

solution, QENS experiments resolve one dominant time-scale over all measured temperatures, while for the 1M NALMA in glycerol:H_2O solution, experiments resolve a faster relaxation with a lower activation energy, as well as a slower relaxation with a significantly larger and growing activation energy. In our simulations, by separating the water molecules into bulk-like and surface water populations, we can follow the dynamics of water in different hydration layers of the peptide. This analysis found a distinct separation in both translation and rotational relaxation times for water in the 1M NALMA in glycerol:H_2O solution, and only one relaxation time for the 1M NALMA in DMSO:H_2O solution, consistent with experiment. Interestingly, in contrast to the trends observed in a pure NALMA:H_2O solution (no co-solvent) in which the bulk-like water is faster than average, it is now the bulk-like water which relaxes on a slower time scale compared to the water molecules that travel in and out of the surface regions.

To understand the relative slow down of water in the bulk-like region, we turn to our analysis of the hydrogen bond relaxations, in which we find that the longest lived hydrogen bond populations are formed between the water donating protons to either the glycerol or DMSO co-solvent. Thus it appears, in contrast to the pure water solvent, that when the water molecules transition to the peptide surface, the hydrogen bonds they form with the surface are more transient than those formed with the co-solvent molecules in the bulk-like region. Hence diffusion in and out of the surface region can be faster than water remaining in the bulk-like region, first because it will likely require breaking a hydrogen bond to move into the surface region, and second because it can result in a shorter lived interaction with the peptide surface.

While this explanation supports the observation that bulk-like water now diffuses more slowly than the exchange water, it does not isolate why the separation in time scales only occurs in the glycerol solution. Due to the similarities in hydrogen bond population relaxations in both co-solvent solutions (Figure 12), the major remaining difference between the two co-solvent solutions is the presence or absence of hydrophobic regions of the co-solvent molecules themselves. In the 1M NALMA in DMSO:H_2O solution, water molecules encounter hydrophobic regions throughout the solution, whether with DMSO or (more minimally) with the peptide surface, giving rise to a single environment. What is interesting in particular is that the water dynamics in the 1M NALMA in DMSO:H_2O solution are similar to the previously characterized NAGMA in H_2O solution, i.e., only one time-scale is measured in both experiment and simulation. It seems that the amphiphilic DMSO

could be acting much like a detergent, and shielding the hydrophobic leucine group from the water with its own methyl groups such that the surface exposed to the water is more homogeneously polar, like NAGMA. The water molecules in both these solutions then do not encounter as significant changes in chemistry as they move in and out of the surface regions.

In the glycerol solution however, water molecules are relatively densely populated near the hydrophobic region of peptide surface since the water molecules are small enough to form water-water hydrogen bonds (unlike the glycerol co-solvent) while orienting around the hydrophobic side chain. Nowhere else in the NALMA:glycerol:H_2O solution do the water molecules encounter these non-hydrogen bonding regions. These water molecules are then faced with distinct changes in chemical bonding potential in specifically defined localities throughout the fluid. This strain could give rise to the population of more mobile water molecules that have not found an energetically favorable hydrogen bonded structural orientation. This explanation is also consistent with our previous findings for pure peptide:H_2O solutions (no-cosolvents), where only the peptide solution with surface hydrophobic regions (NALMA) gave rise to a separation in time scales, while the solution of water and hydrophilic peptides (NAGMA) did not[28].

Our results imply that a protein stabilizer such as glycerol keeps the peptide surface hydrated, even more so than in the pure water, such that the water molecules in solutions are able to reproduce the dynamics signatures observed in the pure water solvent. The denaturing DMSO restricts the water's access to the peptide surface, particularly near hydrophobic regions, and as a result also disrupts the dynamic properties of the water. This detergent-like ability of DMSO to effectively make a NALMA peptide appear like a NAGMA peptide could be a useful property for protein control or design. Interesting further studies could investigate the concentrations effects on structure and dynamics and whether other stabilizing agents besides glycerol also give rise to the two time scales, which may be a more universal feature of water near a stable protein.

ACKNOWLEDGMENTS

We gratefully acknowledge the support of the National Science Foundation and NERSC for computational resources.

REFERENCES

(1) Bondos, S. E.; Bicknell, A. *Analytical Biochemistry* **2003**, *316*, 223.

(2) Dellerue, S.; Petrescu, A. J.; Smith, J. C.; Bellissent-Funel, M. C. *Biophysical Journal* **2001**, *81*, 1666.

(3) Wang, W. *Int. J. of Pharmaceuticals* **1999**, *185*, 129.

(4) Rivas, G.; Fernandez, J. A.; Minton, A. P. *PNAS* **2000**, *98*, 3150.

(5) Timasheff, S. N. *Annu Rev Biophys. Biomol. Struct.* **1993**, *22*, 67.

(6) Tanford, C. *Adv Protein Chem* **1970**, *24*, 1.

(7) Casassa, E. F.; Eisenberg, H. *Adv Protein Chem* **1964**, *19*, 287.

(8) Kirkwood, J. G.; Goldberg, R. J. *J. Chem. Phys.* **1950**, *18*, 54.

(9) Stockmayer, W. H. *J. Chem. Phys.* **1950**, *18*, 58.

(10) Davis-Searles, P. R.; Saunders, A. J.; Erie, D. A.; Winzor, D. J.; Pielak, G. J. *Annu Rev Biophys. Biomol. Struct.* **2001**, *30*, 271.

(11) Almarsson, O.; Kilbanov, A. M. *Biotech and Bioeng.* **1996**, *49*, 87.

(12) Shoichet, B. K.; Baase, W. A.; Kuroki, R.; Matthews, B. *PNAS* **1995**, *92*, 452.

(13) Rupley, J. A.; Yanh, P. H.; Tollin, G. *Symposium Series Am. Chem. Soc., Washington DC* **1980**, *127*, 111.

(14) Angell, C. A. *Science* **1995**, *267*, 1924.

(15) Chen, S. H.; Liu, L.; Fratini, E.; Baglioni, P.; Faraone, A.; Mamontov, E. *Proc Natl Acad Sci U S A* **2006**, *103*, 9012.

(16) Tournier, A. L.; Xu, J.; Smith, J. C. *Biophysical Journal* **2002**, *85*, 1871.

(17) Vitkup; Ringe, D.; Petsko; Karplus, M. *Nat. Struct. Bio* **2000**, *7*, 34.

(18) Tarek, M.; Tobias, D. J. *Eur. Biophys. J* **2008**, *37*, 701.

(19) Halle, B. *Philos Trans R Soc Lond B Biol Sci* **2004**, *359*, 1207.

(20) Pizzitutti, F.; Marchi, M.; Sterpone, F.; Rossky, P. J. *J Phys Chem B* **2007**, *111*, 7584.

(21) Halle, B.; Anderssen, T.; Forsen, S.; Lindman, B. *JACS* **1981**, *103*, 500.

(22) Marchi, M.; Sterpone, F.; Ceccarelli, M. *JACS* **2002**, *124*, 6787.

(23) Gekko, K.; Timasheff, S. N. *Biochemistry* **1981**, *20*, 4667.

(24) Correa, F.; Farah, C. S. *Biophysical Journal* **2007**, *92*, 2463.

(25) Rariy, R. V.; Klibanov, A. M. *Proceedings of the National Academy of Sciences of the United States of America* **1997**, *94*, 13520.

(26) Tjernberg, A.; Markova, N.; Griffiths, W. J.; Hallen, D. *J. Biomol. Screening* **2006**, *11*, 131.

(27) Arakawa, T.; Kita, Y.; Timasheff, S. N. *Biophys. Chem* **2007**, *131*, 62.

(28) Johnson, M. E.; Malardier-Jugroot, C.; Murarka, R.; Head-Gordon, T. *J. Phys. Chem. B* **2009**, *113*, 4082.

(29) Malardier-Jugroot, C.; Johnson, M. E.; Murarka, R. K.; Head-Gordon, T. *Physical Chemistry Chemical Physics* **2008**, *10*, 4903.

(30) Malardier-Jugroot, C.; Head-Gordon, T. *Phys Chem Chem Phys* **2007**, *9*, 1962.

(31) Russo, D.; Murarka, R. K.; Hura, G.; Verschell, E. R.; Copley, J. R. *J Phys Chem B* **2005**, *108*, 19885.

(32) Russo, D.; Murarka, R. K.; Copley, J. R.; Head-Gordon, T. *J Phys Chem B* **2005**, *109*, 12966.

(33) Russo, D.; Hura, G.; Head-Gordon, T. *Biophysical Journal* **2004**, *86*, 1852.

(34) Qvist, J.; Halle, B. *J. Am. Chem. Soc* **2008**, *130*, 10345.

(35) Malardier-Jugroot, C.; Johnson, M. E.; Bowron, D.; Soper, A. K.; Head-Gordon, T. *Phys Chem Chem Phys* **2009**, *submitted*.

(36) Ren, P.; Ponder, J. *J Phys Chem B* **2003**, *107*, 5933.

(37) Case, D. A.; Darden, T. A.; T.E. Cheatham, I.; Simmerling, C. L.; Wang, J.; Duke, R. E.; Luo, R.; Crowley, M.; Walker, R. C.; Zhang, W.; Merz, K. M.; B.Wang; Hayik, S.; Roitberg, A.; Seabra, G.; Kolossváry, I.; K.F.Wong; Paesani, F.; Vanicek, J.; X.Wu; Brozell, S. R.; Steinbrecher, T.; Gohlke, H.; Yang, L.; Tan, C.; Mongan, J.; Hornak, V.; Cui, G.; Mathews, D. H.; Seetin, M. G.; Sagui, C.; Babin, V.; Kollman, P. A. *Univ of California, San Francisco* **2008**.

(38) Ren, P.; Ponder, J. W. *J Phys Chem B* **2004**, *108*, 13427.

(39) Ponder, J.; Case, D. *Adv Protein Chem* **2003**, *66*, 27.

(40) Frisch, M. J., G. W. Trucks, H. B. Schlegel, G. E. Scuseria, M. A. Robb, J. R. Cheeseman, J. A. Montgomery, Jr., T. Vreven, K. N. Kudin, J. C. Burant, J. M. Millam, S. S. Iyengar, J. Tomasi, V. Barone, B. Mennucci, M. Cossi, G. Scalmani, N. Rega, G. A. Petersson, H. Nakatsuji, M. Hada, M. Ehara, K. Toyota, R. Fukuda, J. Hasegawa, M. Ishida, T. Nakajima, Y. Honda, O. Kitao, H. Nakai, M. Klene, X. Li, J. E. Knox, H. P. Hratchian, J. B. Cross, V. Bakken, C. Adamo, J. Jaramillo, R. Gomperts, R. E. Stratmann, O. Yazyev, A. J. Austin, R. Cammi, C. Pomelli, J. W. Ochterski, P. Y. Ayala, K. Morokuma, G. A. Voth, P. Salvador, J. J. Dannenberg, V. G. Zakrzewski, S. Dapprich, A. D. Daniels, M. C. Strain, O. Farkas, D. K. Malick, A. D. Rabuck, K. Raghavachari, J. B. Foresman, J. V. Ortiz, Q. Cui, A. G. Baboul, S. Clifford, J. Cioslowski, B. B. Stefanov, G. Liu, A. Liashenko, P. Piskorz, I. Komaromi, R. L. Martin, D. J. Fox, T. Keith, M. A.

Al-Laham, C. Y. Peng, A. Nanayakkara, M. Challacombe, P. M. W. Gill, B. Johnson, W. Chen, M. W. Wong, C. Gonzalez, and J. A. Pople. Gaussian 03 Revision C.02; Gaussian, I., Ed. Wallingford, CT, 2004.

(41) Stone, A. J. *Chem. Phys Lett* **1981**, *83*, 233.

(42) Stone, A. J. **2003**, *GDMA V2.2.03*.

(43) Ren, P.; Ponder, J. *J. Comput. Chem* **2002**, *23*, 1497.

(44) Lii, J.-H.; Allinger, N. L. *J. Comput. Chem* **1991**, *12*, 186.

(45) Shao, Y., L. Fusti-Molnar, Y. Jung, J. Kussmann, C. Ochsenfeld, S. T. Brown, A. T. B. Gilbert, L. V. Slipchenko,S. V. Levchenko, D. P. O'Neill, R. A. Distasio Jr., R. C. Lochan, T. Wang, G. J. O. Beran, N. A. Besley, J. M., Herbert, C. Y. Lin, T. Van Voorhis, S. H. Chien, A. Sodt, R. P. Steele, V. A. Rassolov, P. E. Maslen, P. P. Korambath, R. D. Adamson, B. Austin, J. Baker, E. F. C. Byrd, H. Dachsel, R. J. Doerksen, A. Dreuw, B. D. Dunietz, A. D. Dutoi, T. R. Furlani, S. R. Gwaltney, A. Heyden, S. Hirata, C.-P. Hsu, G. Kedziora, R. Z. Khalliulin, P. Klunzinger, A. M. Lee, M. S. Lee, W. Liang, I. Lotan, N. Nair, B. Peters, E. I. Proynov, P. A. Pieniazek, Y. M. Rhee, J. Ritchie, E. Rosta, C. D. Sherrill, A. C. Simmonett, J. E. Subotnik, H. L. Woodcock III, W. Zhang, A. T. Bell, A. K. Chakraborty, D. M. Chipman, F. J. Keil, A. Warshel, W. J. Hehre, H. F. Schaefer III, J. Kong, A. I. Krylov, P. M. W. Gill, M. Head-Gordon. *Phys Chem Chem Phys* **2006**, *8*, 3172.

(46) Hansen, J. P.; McDonald, I. R. *Theory of Simple Liquids*, 3rd ed.; Academic Press: London, 2006.

(47) Palmer, R. G.; Stein, D. L.; Abrahams, E.; Anderson, P. W. *Phys Rev Lett* **1984**, *53*, 957.

(48) Zanotti, J. M.; Bellisent-Funel, M. C.; Chen, S. H. *Phys Rev E* **1999**, *53*, 3084.

(49) Sears, V. F. *Canadian Journal of Physics* **1967**, *45*, 237.

(50) Chen, S. H.; Gallo, P.; Sciortino, F.; Tartaglia, P. *Physical Review E* **1997**, *56*, 4231.

(51) Luzar, A.; Chandler, D. *Nature* **1996**, *379*, 55.

(52) Ferrario, M.; Haughney, M.; McDonald, I. R.; Klein, M. L. *J. Chem. Phys.* **1990**, *93*, 5156.

(53) Hura, G.; Sorenson, J. M.; Glaeser, R. M.; Head-Gordon, T. *Perspectives in Drug Discovery & Design* **1999**, *17*, 97.

(54) Soper, A. K.; Luzar, A. *J. Chem. Phys.* **1992**, *97*, 1320.

(55) Cabral, J. T.; Luzar, A.; Teixeira, J.; Bellissent-Funel, M. C. *J. Chem. Phys.* **2000**, *113*, 8736.

TABLES

Table 1. Intermediate scattering function (ISF) fit parameters, τ (Eq. (4)) and $\overline{\tau}$ (Eq. (5)), for water:co-solvent and NALMA and water:co-solvent solutions at Q=0.954A^{-1} at T=298K and T=263K.

	T=298K				***T=263K***			
Solution	***A***	***τ (ps)***	***β***	$\overline{\tau}$ ***(ps)***	***A***	***τ (ps)***	***β***	$\overline{\tau}$ ***(ps)***
H_2O Glycerol	0.97	62.1	0.72	76.6	0.95	1463	0.65	2003
NALMA/Glycerol	0.94	84.4	0.69	108.3	0.96	1356	0.61	1997
H_2O DMSO	0.92	96.9	0.79	110.4	0.95	1968	0.65	2689
NALMA/DMSO	0.93	101	0.73	123	0.93	2027	0.7	2566

FIGURE CAPTIONS

Figure 1: *Site−site radial distribution function $g_{CC}(r)$ of the intermolecular NALMA methyl carbons in DMSO (continuous lines) and glycerol (dotted lines) at 298K.* No clustering of the NALMA molecules is observed with or without co-solvents.

Figure 2: *Site−site radial distribution function $g_{HC}(r)$ of the water hydrogen atom around the carbon of the carbonyl group of NALMA at 298K.* (a) in pure water solvent, (b) in glycerol, and (c) in DMSO. The red solid line and the black markers indicate that there is some anisotropy between the two carbonyl groups (which do not have perfectly symmetric bonding groups). Experimentally, the coordination number for $g_{HC}(r)$ integrated to 3.1Å is 1.1 for 1M NALMA and 1.0 for 1M NALMA in glycerol:H_2O, but is close to zero for 1M NALMA in 1:4 DMSO:H_2O. By contrast, the simulations maintain the hydrogen-bond in all three solutions.

Figure 3: *Spatial distribution functions of water oxygen atoms around the hydrophobic leucine side chain*. (a) 1M NALMA without co-solvent, (b) 1M NALMA in 1:5 glycerol:H_2O, and (c) 1M NALMA in 1:4 DMSO:H_2O. Result is calculated with Eq. (11) where a leucine delta Carbon is the origin (gray atom), the z-axis is set by the same methyl hydrogen (gold atom), and the x-plane is set by the gamma Carbon (purple atom). The density was plotted over the range 2.0–4.7 Å, where a value of 1 indicates the average water density, and the highest density values reached are plotted. The maximum density with glycerol present is 4, compared to only 2.5 with no co-solvent.

Figure 4: *Spatial distribution functions of the water oxygen atoms around a central water molecule.* Origin is given by the central water oxygen, and z-axis is set by OH_1 bond, with x-plane set by the OH_2 bond. (a) 1M NALMA without co-solvent, (b) 1M NALMA in 1:5 glycerol:H_2O, and (c) 1M NALMA in 1:4 DMSO:H_2O. The density was plotted in the range 2.1-4.7Å (the first water coordination shell).

Figure 5: *Site-Site radial distribution function between the water oxygens and co-solvent oxygen atoms at 298K.* 1M NALMA solution with 1:5 glycerol:H_2O solution (blue dotted line) and the 1M NALMA solution with 1:4 DMSO:H_2O solution (red solid line). The orientational spatial distribution further shows that these contacts are sharply defined along the water OH axes,

indicating hydrogen bonding. The rigidity of the DMSO bond could explain the disagreement between diffraction data and simulation at the peptide backbone surface seen in Figure 2.

Figure 6: *Simulation and experimental data of D_{trans} vs. T^{-1} for water in the presence of the DMSO co-solvent with and without NALMA.* (a) 1:4 DMSO:H_2O for temperatures between 263K and 298K. Using Eq. (2,) E_A= 11.9kcal/mol for simulation and 6.5kcal/mol for experiment (b) 1M NALMA in 1:4 DMSO:H_2O solution for temperatures between 255K and 298K. E_A=12kcal/mol for simulation and 7.0 kcal/mol for experiment. Simulated and experimental values (symbols) and Arrhenius fit (Eq. (2); solid line). For both plots experimental data extends to 230K.

Figure 7: *Simulation and experimental data of D_{trans} vs T^{-1} for water in the presence of the glycerol co-solvent with and without NALMA.* (a) 1:5 glycerol:H_2O for temperatures between 263K and 298K. Using Eq. (2,) E_A= 11.7kcal/mol for simulation and 7.3kcal/mol for experiment. (b) 1M NALMA in 1:5 glycerol:H_2O solution for temperatures between 255K and 298K. E_A=11.2kcal/mol for simulation and 5.8kcal/mol for the data between 298K-263K. Simulated and experimental values (symbols) and Arrhenius fit (Eq. (2); solid line). For both plots experimental data extends to 235K.

Figure 8: *Intermediate scattering function obtained from the MD simulations (symbols) and fit obtained with a stretched exponential function (black line).* (a) 1:5 Glycerol:H_2O at 298K, (b) 1M NALMA in 1:5 glycerol:H_2O solution at 298K. (c) 1:5 Glycerol:H_2O at 263K, (d) 1M NALMA in 1:5 glycerol:H_2O solution at 263K

Figure 9. *Populations of water molecules found near the NALMA peptide surface and "bulk" regions as a function of time for different temperatures.* (a) 1M NALMA in 1:5 glycerol:H_2O solution, and (b) 1M NALMA in 1:4 DMSO:H_2O solution. Solid lines are the bulk water, dashed lines are the hydration layer transfer water.

Figure 10. *Mean square displacement (MSD) as a function of time for populations of water molecules found in the hydration layer and bulk regions at 263K.* (a) 1M NALMA in 1:5 glycerol:H_2O solution and (b) 1M NALMA in 1:4 DMSO:H_2O solution.

Figure 11: *Intermediate scattering function (ISF, solid lines) for* $Q=0.9538A^{-1}$ *and rotational correlation functions (RCF, dashed lines) for* $C_{l=1}(t)$*, at 263K.* (a) ISF and RCF for 1M NALMA in 1:5 glycerol:H_2O solution. (b) ISF and RCF for 1M NALMA in 1:4 DMSO:H_2O solution. The rotational correlations are plotted with dashed lines at a constant offset of 0.1 from their actual values.

Figure 12: *Hydrogen bond population auto-correlation functions, B(t), for water at 263K for (a)* 1M NALMA in 1:5 glycerol:H_2O solution, and (b) 1M NALMA in 1:4 DMSO:H_2O solution. Relaxation profiles for bonds formed between pairs of water molecules (blue solid), between water donating a hydrogen to the co-solvent oxygen (red dot-dashed), and between water donating a hydrogen to the NALMA carbonyl oxygen (black dashed).

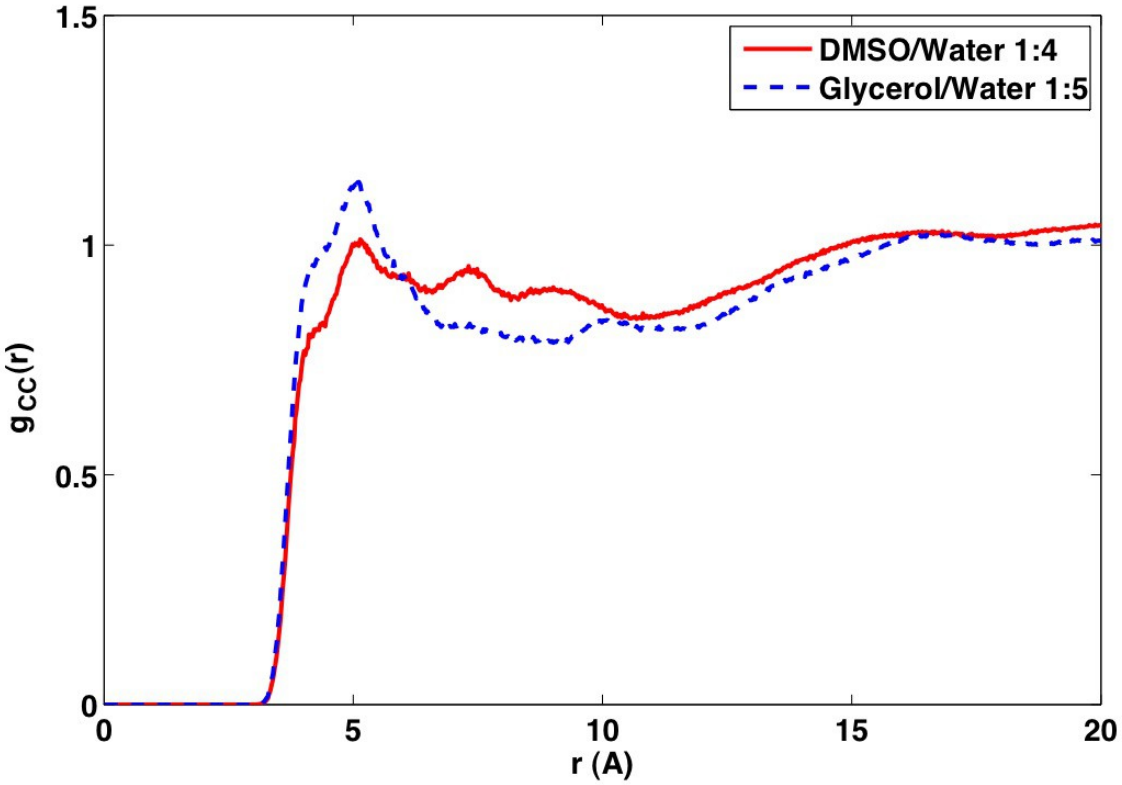

Figure 1. Johnson and co-workers

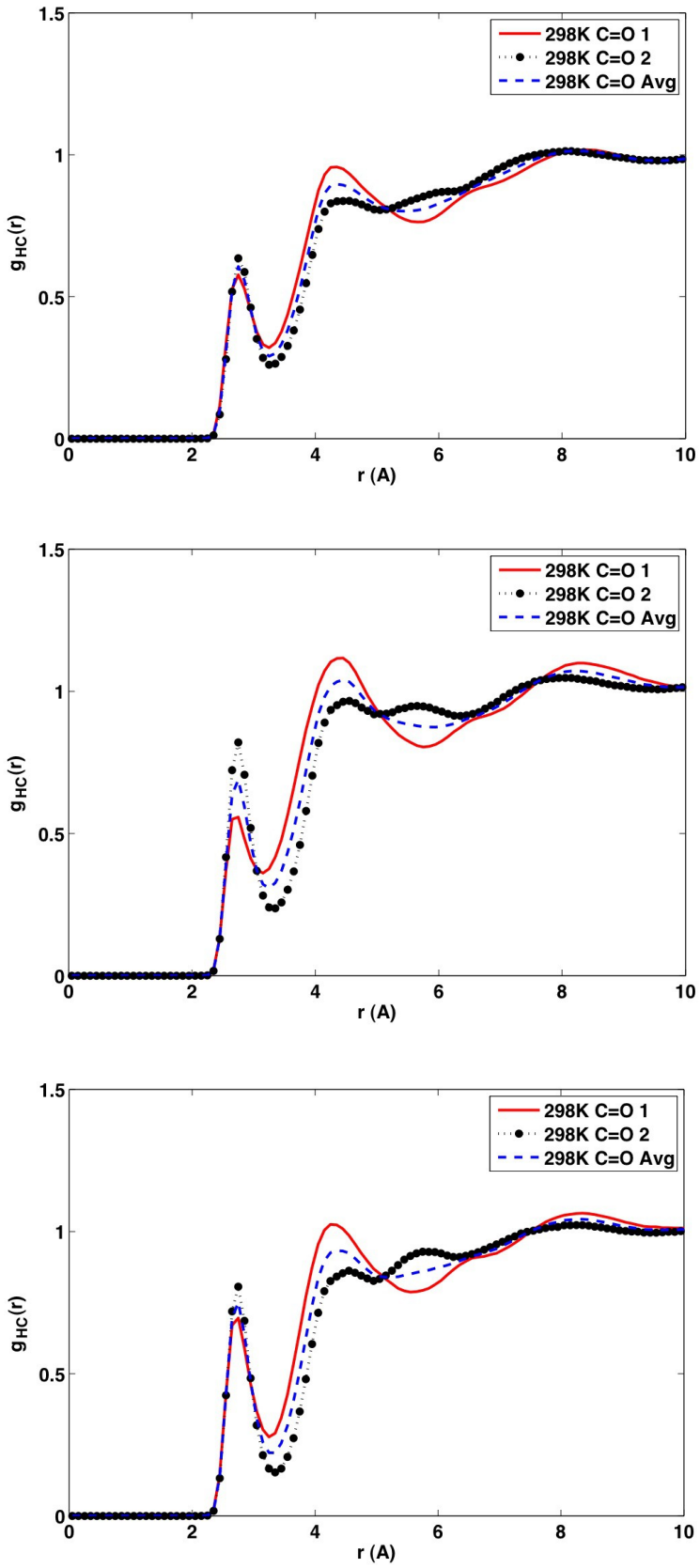

Figure 2. Johnson and co-workers

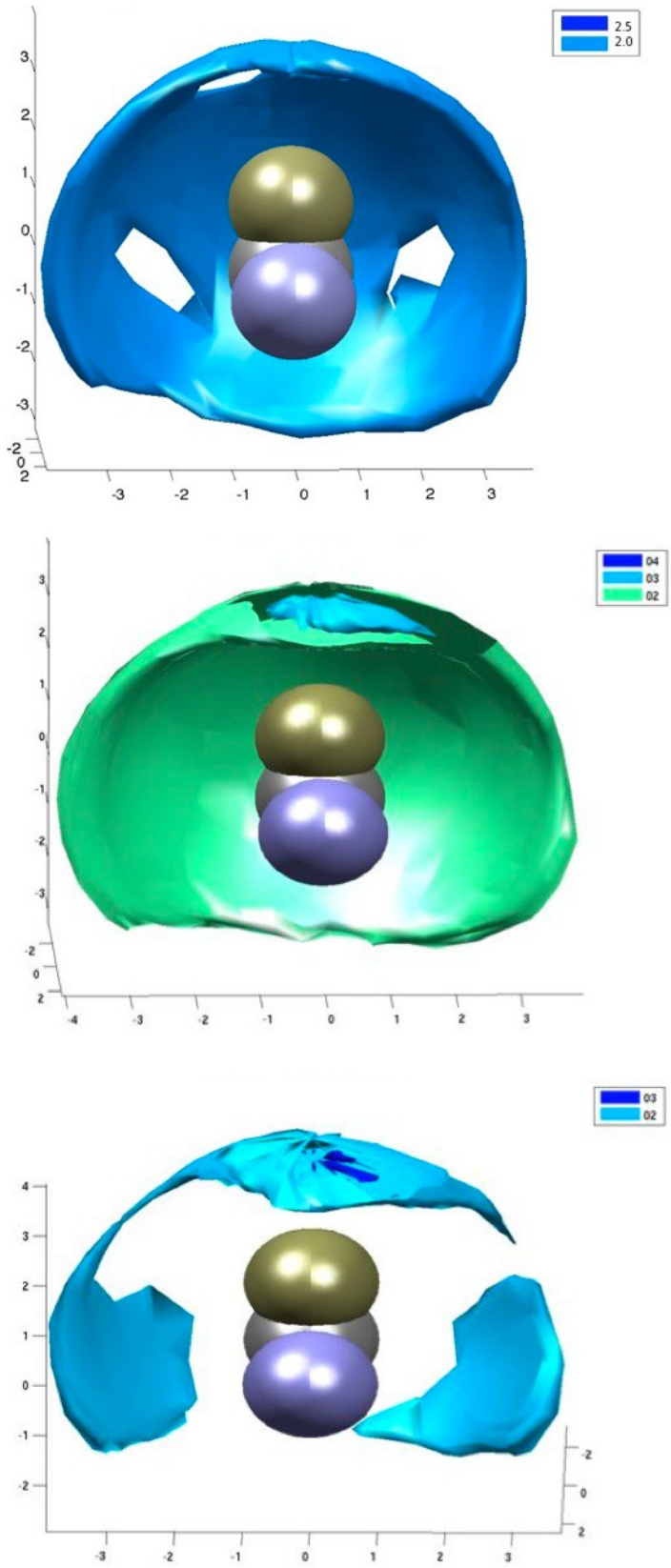

Figure 3. Johnson and co-workers

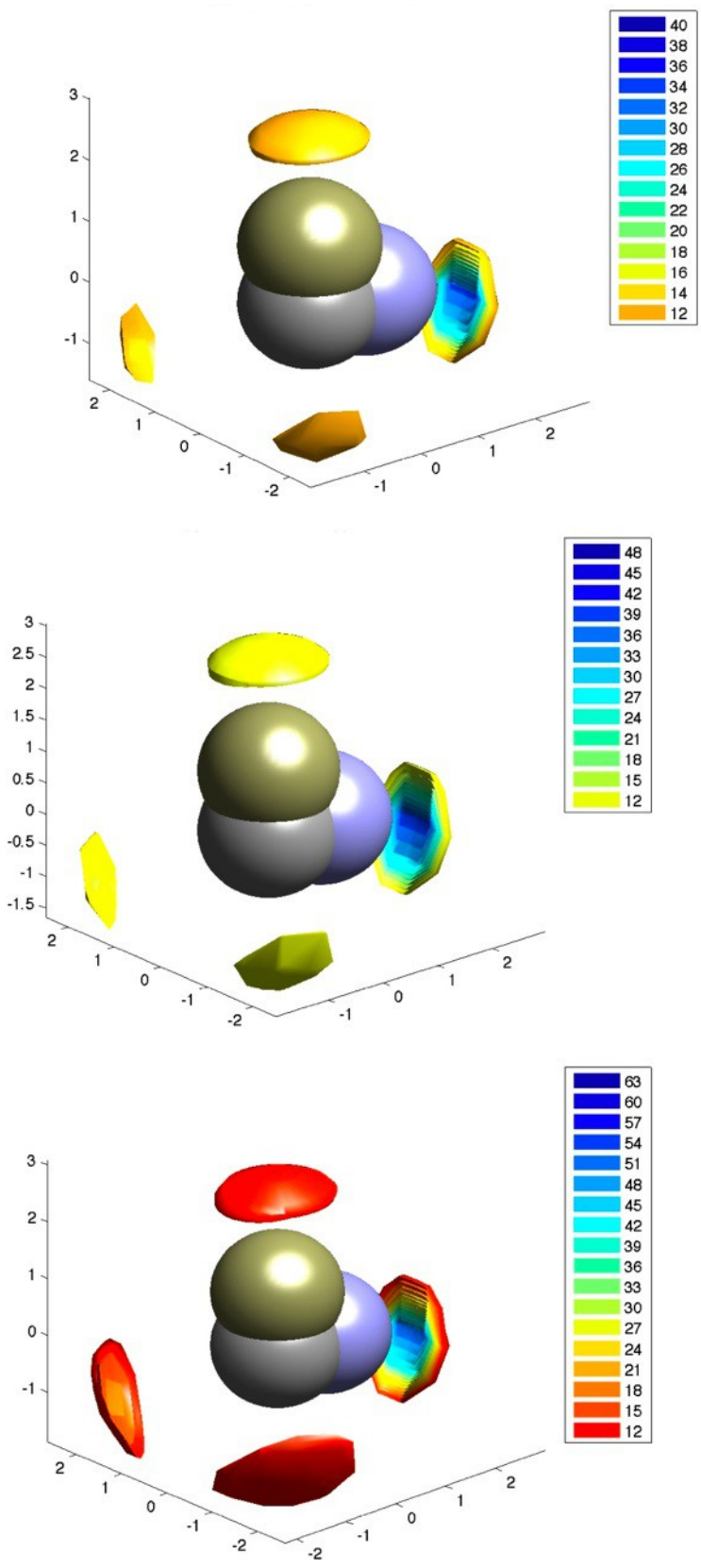

Figure 4. Johnson and co-workers

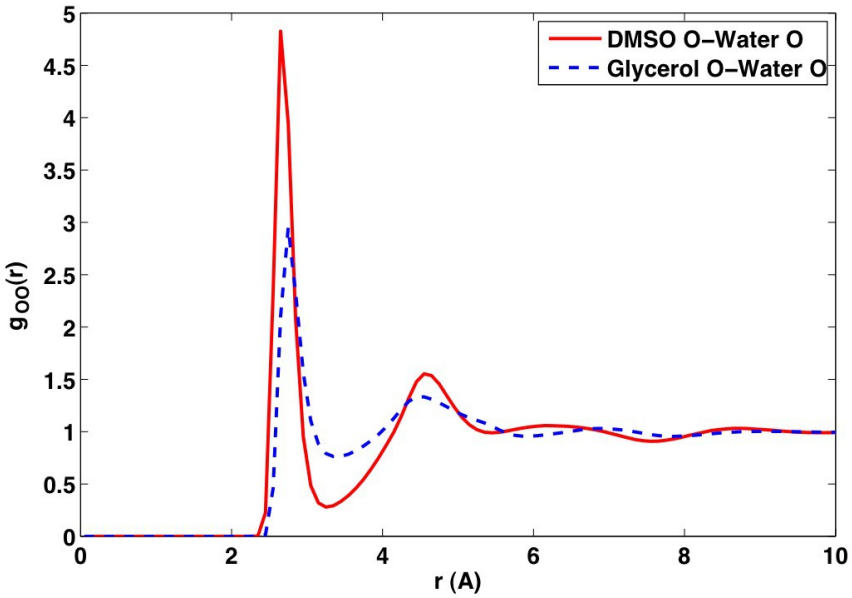

Figure 5. Johnson and co-workers

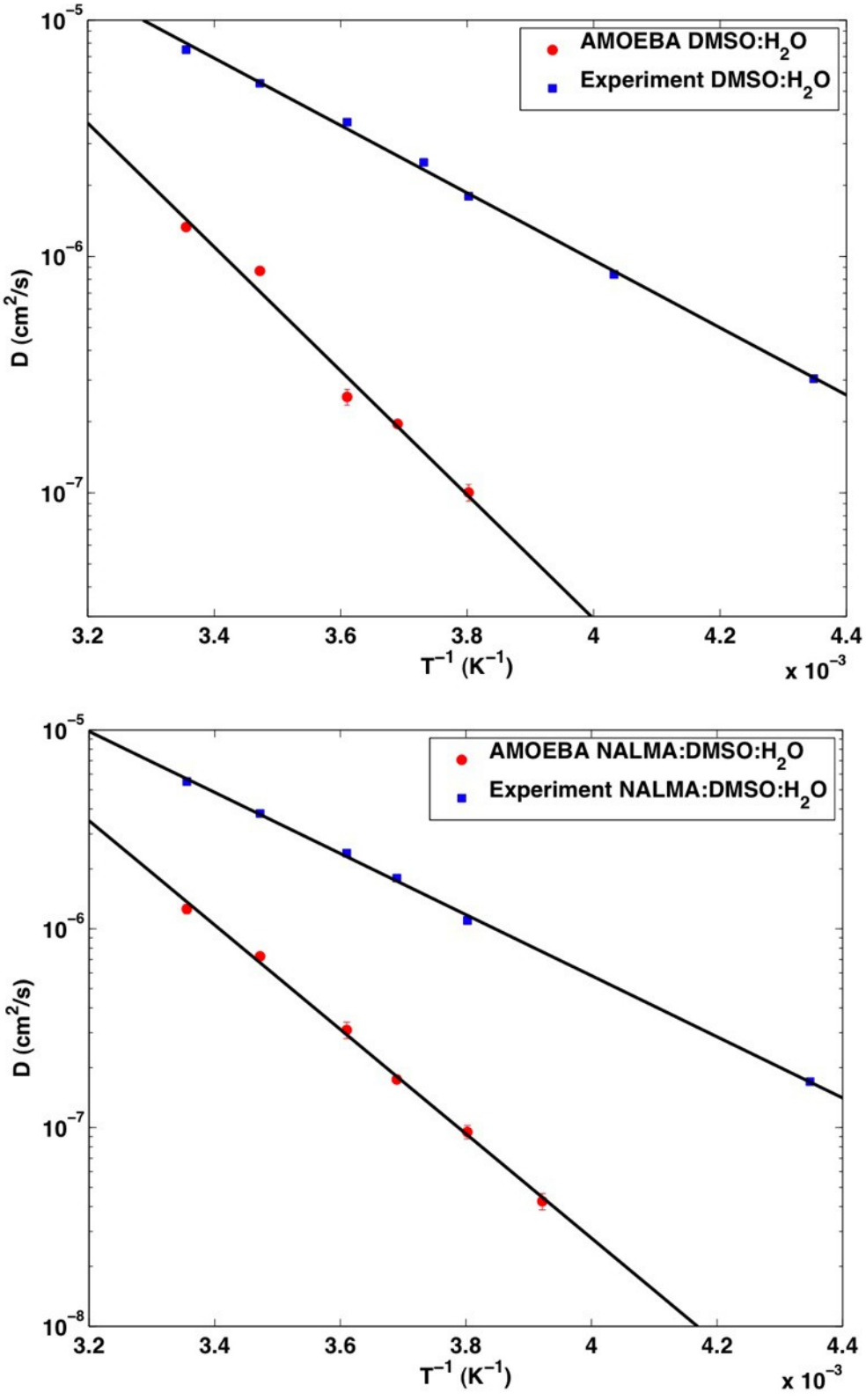

Figure 6. Johnson and co-workers

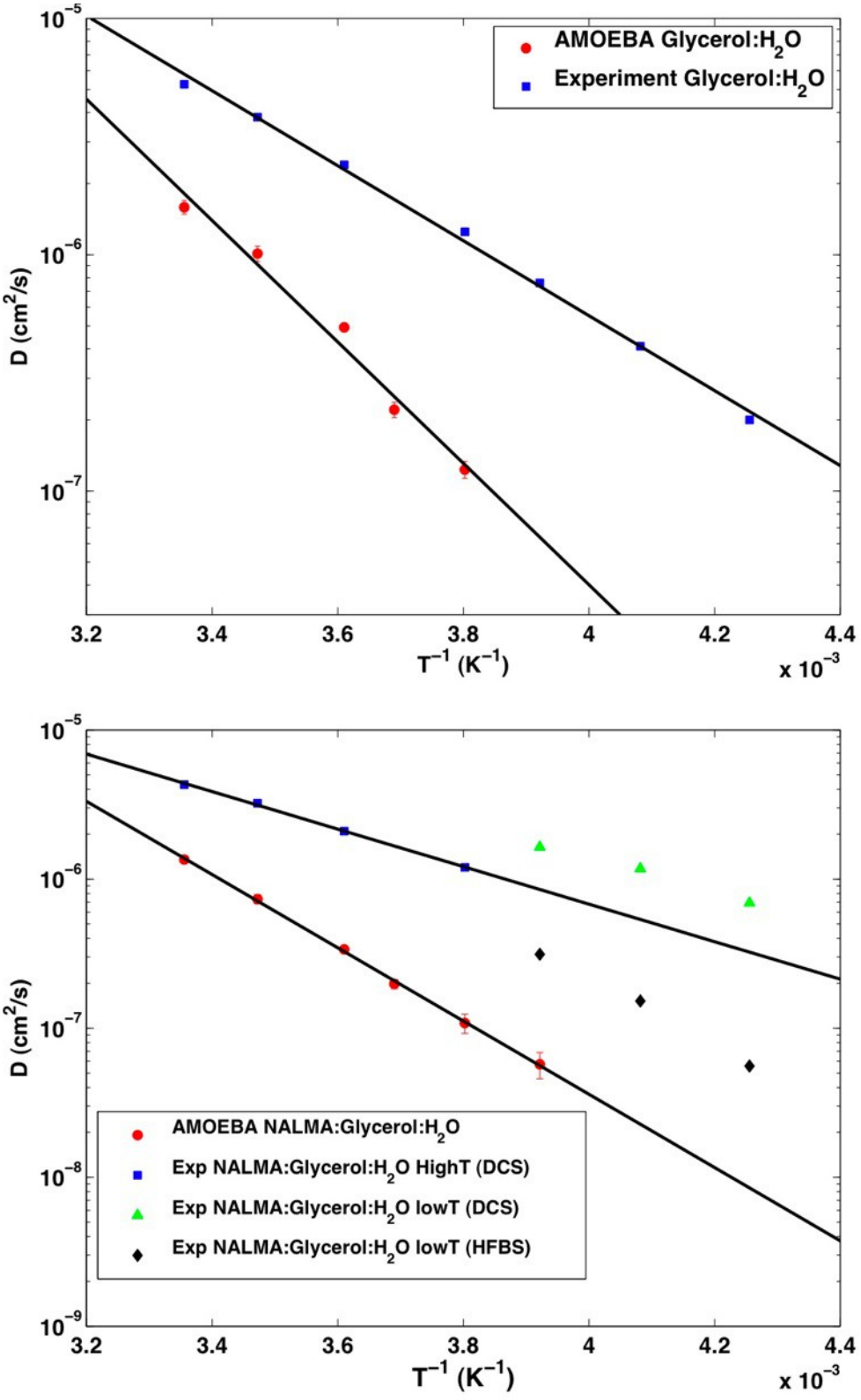

Figure 7. Johnson and co-workers

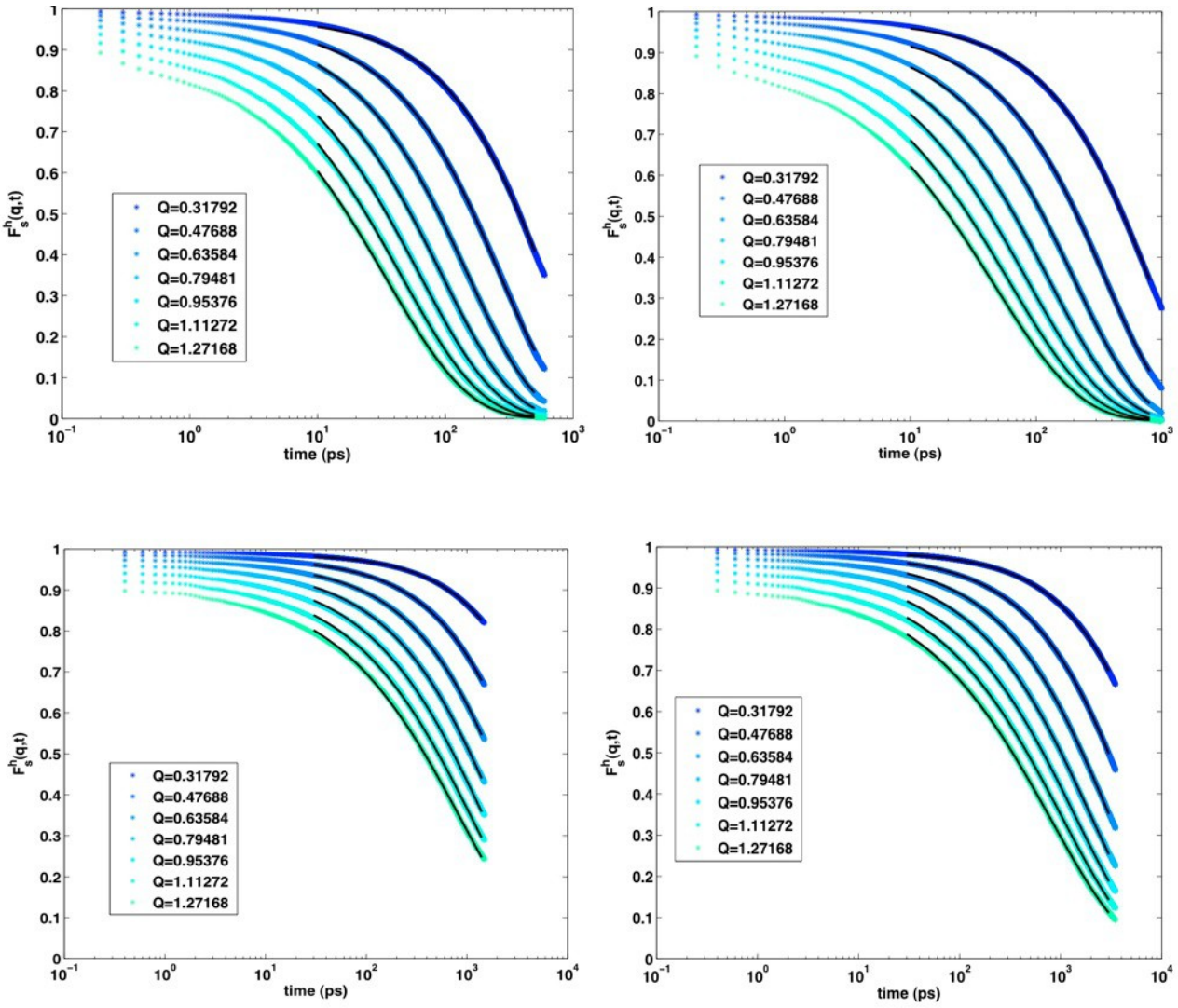

Figure 8. Johnson and co-workers

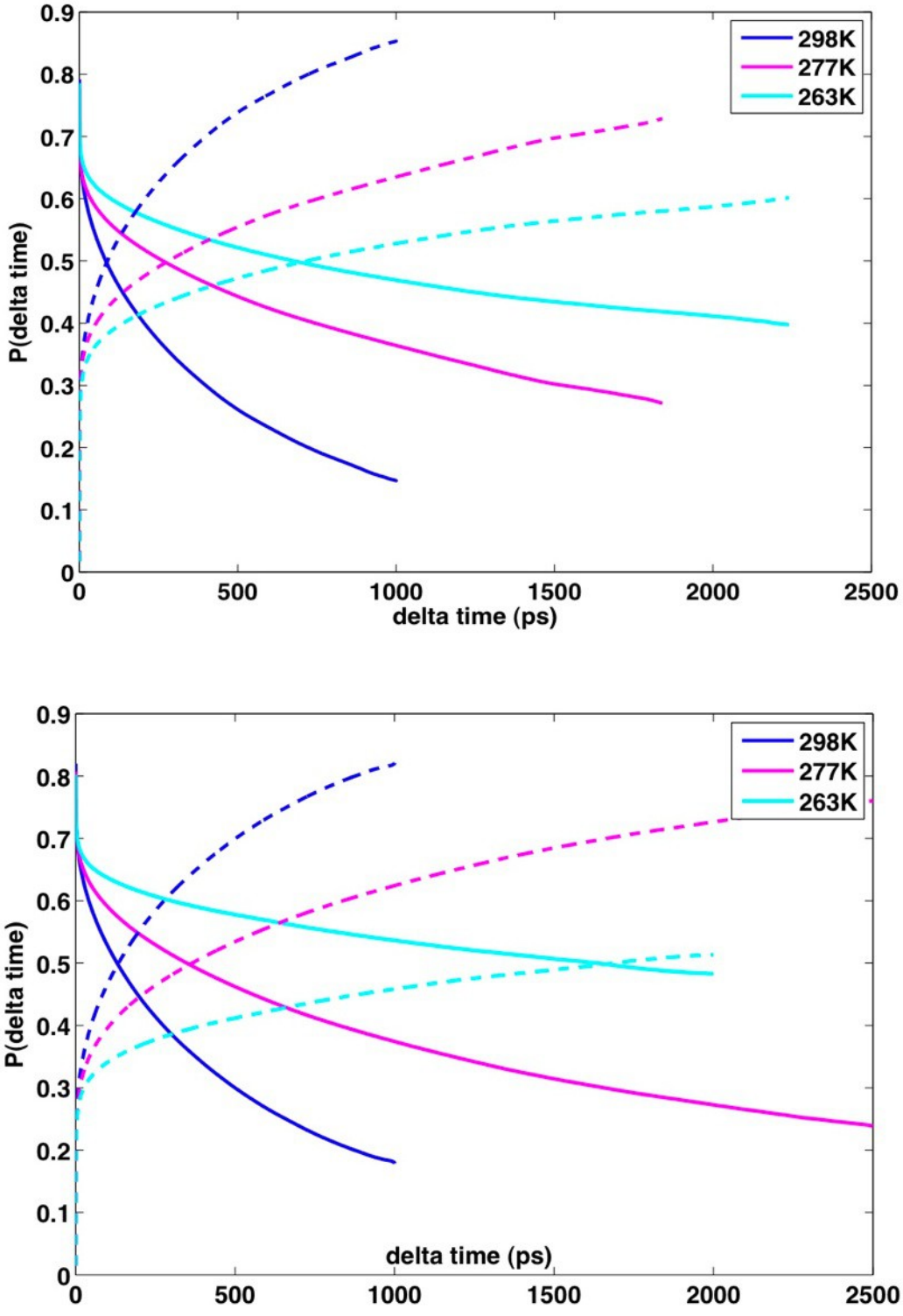

Figure 9. Johnson and co-workers

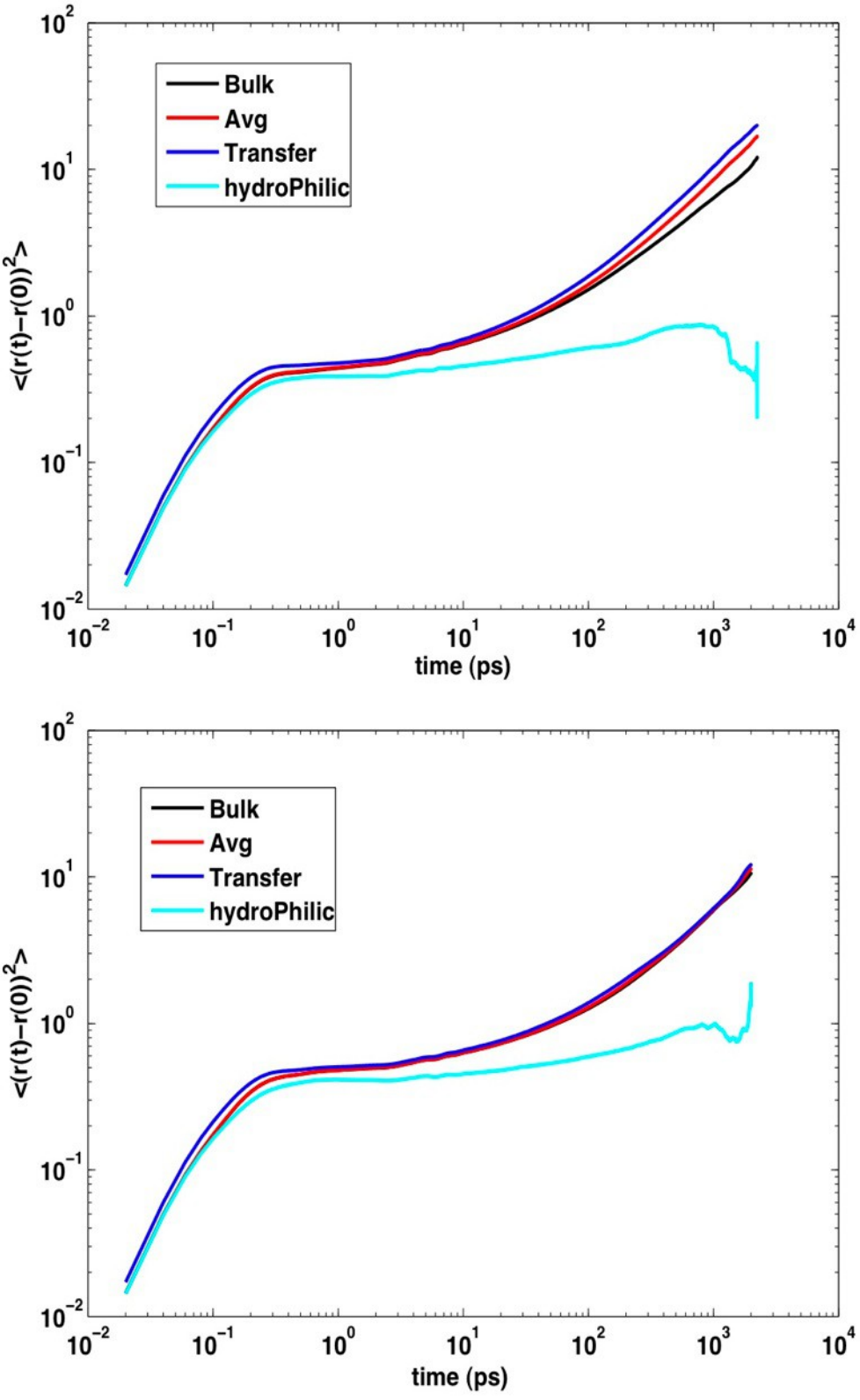

Figure 10. Johnson and co-workers

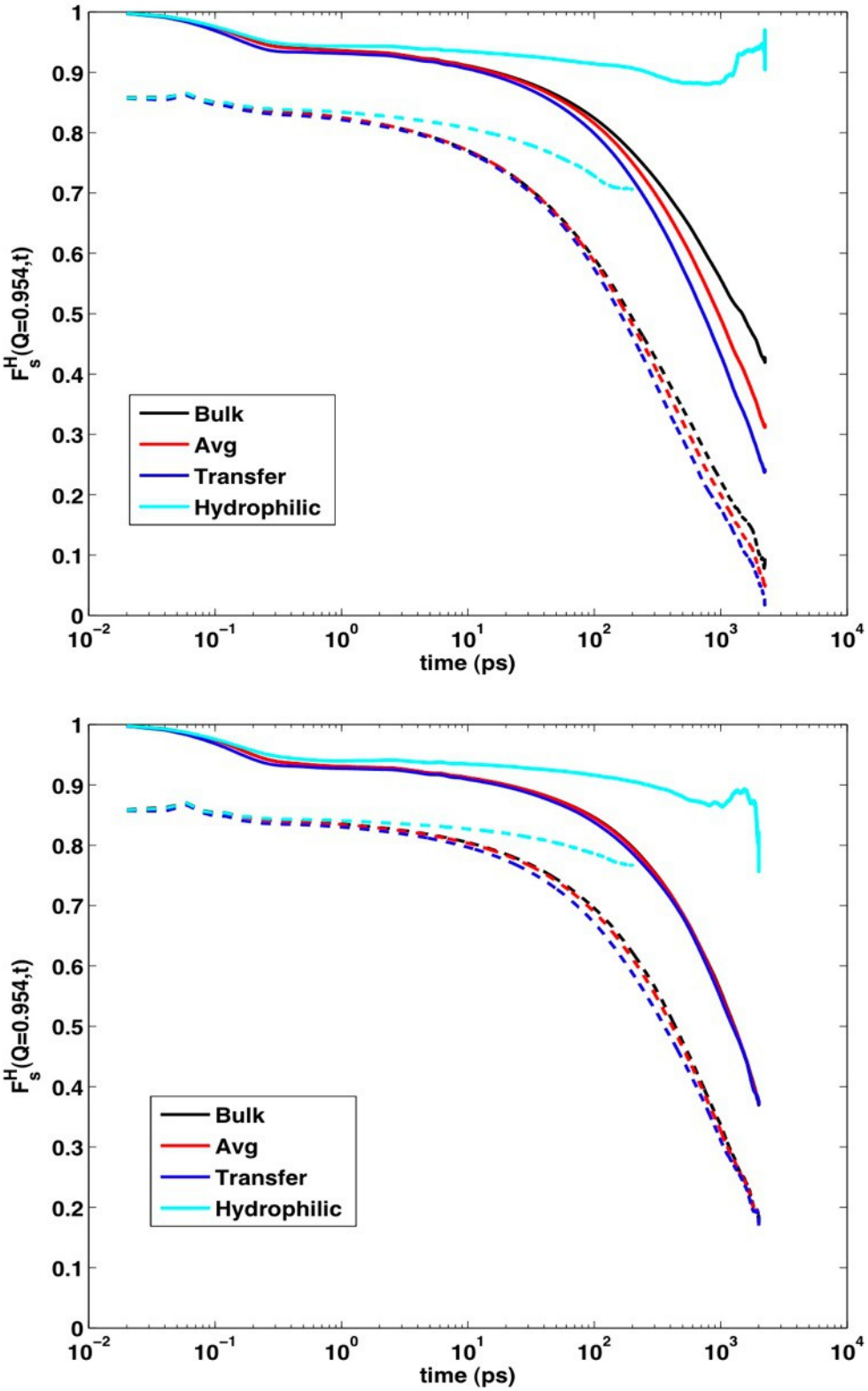

Figure 11. Johnson and co-workers

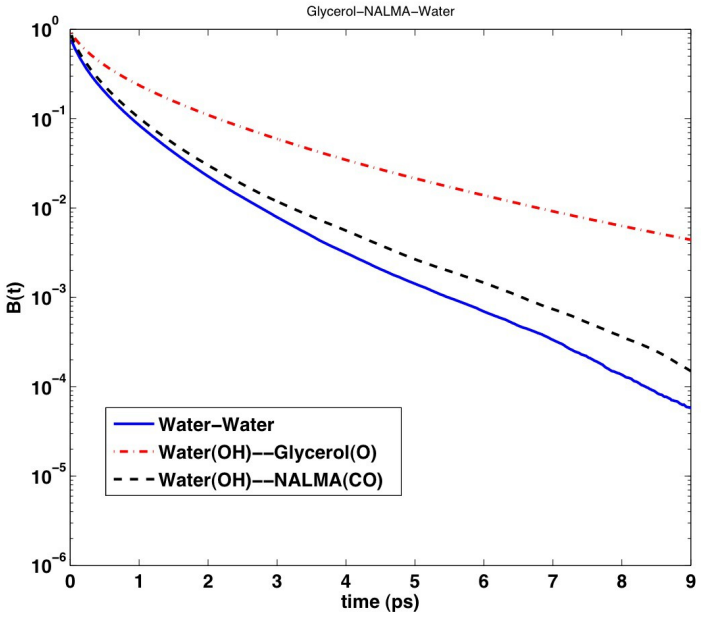
Glycerol–NALMA–Water
B(t)
time (ps)
Water–Water
Water(OH)––Glycerol(O)
Water(OH)––NALMA(CO)

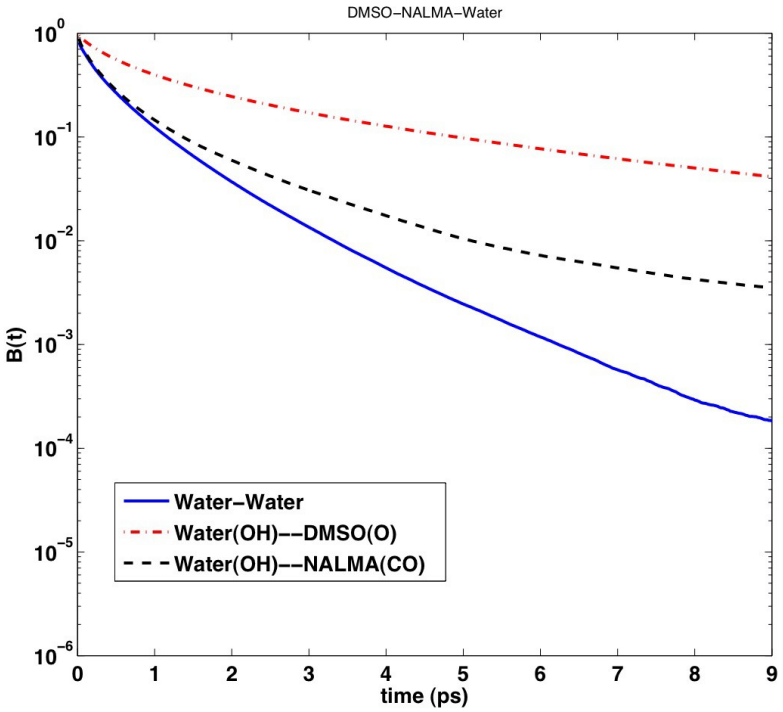

Figure 12. Johnson and co-workers